



Waffle Slab Behavior Subjected to Blast Load

Gorji Bandpey, Gh.¹, Abdollahzadeh, G.R.^{2*} and Firoozjaee, A.R.³

¹ Ph.D. Student, Faculty of Civil Engineering, Babol Noshirvani University of Technology, Babol, Iran.

² Professor of Civil Engineering, Babol Noshirvani University of Technology, Babol, Iran.

³ Associate Professor, Faculty of Civil Engineering, Babol Noshirvani University of Technology, Babol, Iran.

© University of Tehran 2021

Received: 02 Apr. 2020;

Revised: 13 Jun. 2020;

Accepted: 29 Jun. 2020

ABSTRACT: Over the previous years, the use of structure roof systems which can be implemented with long column spans has been welcomed by manufacturers. One of the most widely used roofs is the waffle slab system. Therefore, by reviewing previous studies in the field of roof collapse in reinforced concrete structures under blast, the absence of studies on the performance of waffle slab and comparing its behavior with blast affected RC slabs is observed. Laboratory simulation of this problem requires high cost, high accuracy in model building and much time. In this study, after preliminary model validation with experimental research and two numerical studies in LS-DYNA software, the behavior of waffle slab subjected to blast load and compare its performance with RC slab are investigated. It should be noted that because the blast load is applied to the structure in a very short time, it has a high loading rate. Therefore, the strain rate effects on concrete and reinforcement are considered for achieving real material behavior. The identical volume of concrete and reinforcement used in all roofs is considered in order to evaluate and compare the behavior of the roofs reasonably. Then, the effect of the geometric dimension of waffle molds and the effect of the supporting condition on the Waffle slab responses are studied. Other investigated parameter in this study includes the effect of concrete compressive strength on the behavior of roof under blast load. The mass of the explosive and its distance from the roof surface are other parameters considered in this study. The effect of bar size on the behavior of the roof is also investigated. The results of this study are presented as diagrams and tables showing that given the same volume of concrete and reinforcement in the RC slab and the waffle slab, the central displacement of Waffle slab is reduced to a desirable level. This shows the better behavior of the waffle slab in comparison with the RC slab with the same volume of material under the blast load.

Keywords: Blast Load, Central Displacement, Geometrical Dimension of the Waffle, RC Slab, Strain Rate, Waffle Slab.

* Corresponding author E-mail: g.abdollahzadeh@ymail.com

1. Introduction

Structures are generally designed on the basis of conventional loads, including dead, live, snow, wind and seismic loads, and unconventional loads such as impact, fire and blast are not considered in structural analysis and design. Therefore, during the exposure of the structure to such unusual loads, there would be a great deal of destruction and damage. An example of such damage in recent years in some structures around the world is the twin towers of the World Trade Organization in 2001 collapsed in effect of aircraft collisions with structures followed by blasts and fires. Other structural damage caused by unconventional loads can be attributed to the overall demolition of the Plasco building in Iran in 2017, part of which has been damaged by fire and consequently the loss of strength to roof elements.

One of the most effective elements in controlling the failures caused by unconventional loads is the structural roof that in the case of losing loading capacity of the roof system will lead to the extension of failure in other floors. Many studies have been conducted by researchers on materials as well as blast loads. Steel and concrete are materials that are widely used in construction projects. Concrete has a better strength to blast load than other materials. Therefore, the behavior of reinforced concrete slab due to abnormal loads such as blast is essential to study. Numerical and experimental studies carried out in this area over the last years.

Wang et al. (2013) in an experimental and numerical study, modeled a square reinforced concrete slab under near-field blast. In this study, the mechanism of slab failure under different amounts of explosive was investigated at the distance of 0.4 m from slab surface. Since the blast phenomenon is a type of high-speed dynamic load, they considered the strain rate effects on the behavior of concrete and steel materials. Results of the numerical and experimental models showed good

agreement in this study. This study also showed that as the explosive content increased, the failure mode changed from the whole slab to local failure.

Zhao and Chen (2013) conducted a dynamic analysis of the failure mechanism of a reinforced concrete slab under blast load. In this study, they considered dimensions of $1000 \times 1000 \times 400$ mm for reinforced concrete slab with three different amounts of explosives and modeled in LS-DYNA software and compared the results of this numerical study with existing experimental studies. This research was able to estimate the failure mechanism of the slab under blast load, and the result of this study showed that the destruction mechanism would change as the explosive volume changed.

Shuaib and Daoud (2015) investigated the failure mode and deformation of square concrete slabs due to blast load. The slabs studied are two-end fixed. They assumed the distance between the blast center and the center of the slab constant, but the weight of the explosive varied in three modes. They also modeled their studies numerically in LS-DYNA software. Two KCC and Winfrith behavioral models were used to model concrete materials. In this study, the blast load was applied to the slab with Lagrangian method. To ensure the validity of this study, the results were compared with an experimental study. Both concrete behavior models (KCC and Winfrith) showed good estimates of actual concrete behavior and slab deformation. To investigate the slab failure mode, the KCC behavior of the concrete was optimally modeled by bending cracks, but this behavior model was not capable to model the local shear behavior, because the Lagrangian method is not able to consider the interaction of open air and concrete slab.

In the RC structures, the concrete compressive strength is important in the behavior of structural element under blast load. So, Abdollahzadeh et al. (2017) considered two models based on Gene Expression Programming (GEP). These

models predict compressive strength of High Strength Concrete (HSC). They considered composition of HSC, as a mixture of six components (water, cement, super-plastisizer, silica fume, fine aggregate and coarse aggregate). The target of the prediction is the 28-day compressive strength value. Results of this study show that the GEP is a good method for the prediction of compressive strength amounts of HSC concerning to the outcomes of the training.

Pandey et al. (2006) investigated the failure of concrete thin slabs against blast load. In this study, they investigated the effect of deterioration and reduction of hardness of material on concrete behavior and presented the mechanism of possible failure in their research. The results of this study were validated with numerical models that showed good agreement.

The missing of an element can lead to the beginning of progressive collapse in a structure. So, finding the location of this element is very important. Therefore, Kheyroddin et al. (2019) investigated about this topic and following GSA and DoD guidelines for finding the key element of symmetric structures with different floor heights, sensitivity analysis was modified. Results of this study showed that the location of the key element was different in the plan and height of the structure in structures with different floor heights.

Eltehaway (2009) conducted a study to investigate the performance of reinforced concrete slab under the impact loads and the effect of Ferro cement against slab surface damage. The result of this research showed that the Ferro cement has high ductility and high strength to dynamic loads including impact. Also, by increasing slab thickness, energy absorption and slab strength will increase.

Augustsson and Harenstam (2010) presented two simplified methods for designing beams and reinforced concrete slabs subjected to blast loads. These two methods include manual calculation based on energy equations and numerical

calculation based on motion equations. Both methods proposed in this study assumed that the structure can be simulated as a degree of freedom system and are valid for elastic, plastic and elastoplastic responses. The result of this study was compared with the result of ADINA finite element software and its validity was confirmed.

Chen et al. (2015) studied the dynamic behavior of a rectangular reinforced concrete beam with simple support under blast load. LS-DYNA finite element software was used for this purpose. Numerical simulation was performed in this study for four groups of reinforced concrete beams. In order to study the behavior of this beam, the maximum displacement, concrete cracking, rebar stress and shear stress of the concrete near the support were investigated and the results were compared with an experimental study.

Xu and Lu (2006) performed the effect of blast on reinforced concrete walls in an analytical study. For this purpose, the wave theory was studied and the strain rate effects on concrete were considered. The studied scenarios included the distance and mass of the explosive. The results showed a good verification with the experimental results related to this research.

Yang et al. (2019) studied the effects of blast on rubber reinforced concrete slab. They considered four types of rubber concrete with different rubber ratios in concrete compositions. This study showed that the tensile failure area of slab concrete in rubber concrete is far less than that of conventional concrete subjected to blast. Finally, rubber-reinforced concrete structural elements exhibited a very favorable behavior against the energy released from large blast.

Zhao et al. (2019) studied the effect of blast on composite slab consisting of concrete, steel plate and stud. For this purpose, three types of slab affected by contact blast were studied experimentally and the mechanism of failure, maximum displacement of slab and its dynamic

responses were investigated. In order to confirm the experimental results, these slabs were simulated in finite element software that the agreement between the failure mechanism and the maximum displacement of the slab indicated the accuracy of the experimental model in this study. The results showed that the composite slab behavior is much better than the conventional concrete slab system under contact blast due to the use of steel plate.

Meng et al. (2019) experimentally and numerically studied environment-friendly geopolymer-reinforced concrete slab under the near-field blast. One of the important aims of this study was investigating the mechanism of destruction and comparing it conventional concrete slab. The results of this study showed that the bars in this type of slab experienced less damage than conventional slabs.

On the other hand, the progressive collapse in the structure will be occur if the slab capacity is lost. Regarding the topic of progressive collapse, Zahrai and Ezoddin (2014) presented an analytical method for calculating progressive collapse potential in typical concrete buildings. They compared four methods for progressive collapse analysis by studying 5 and 10-story intermediate moment-resistant reinforced concrete frame buildings. To evaluate the behavior of RC buildings, three column-removal conditions were performed. Their results showed that dynamic analysis procedures pre sent more accurate results to be performed for progressive collapse determination yielded.

By reviewing previous studies, it is concluded that the alternative load path method is suitable for progressive collapse due to explosion. Tavakoli and KiaKojouri (2015) numerically investigated the steel moment resisting frames for evaluation of fire-induced and threat-independent progressive collapse potential. In this study, number of floors and the location of initial failure were considered. Two different mechanisms were assumed in fire-induced and threat-independent progressive

collapse. While column removal alternative load paths play major role in threat-independent, the weight of the structure above the failure region is the most important parameter in fire-induced progressive collapse.

Rezaie et al. (2018) studied about sudden removal of vertical load-bearing elements such as columns in reinforced concrete buildings structures with different floor plans such as floor plans with and without torsional irregularity as well as geometrical regular and irregular floor plans. They considered column sensitivity and displacement sensitivity indexes to compare different cases of column removal in each model. One of the results of this study was that removing shear walls led to much more critical scenarios than removing columns in building with shear walls. As another result, removing the internal columns was less critical than the external columns.

In recent years, there is no research on the behavior of waffle roofs subjected to the blast loads. The use of waffle roof systems with the potential of implementation with columns at high distances has recently been interested by manufacturers. Therefore, this study will investigate the behavior of waffle slab under blast load and compare its performance with that of conventional reinforced concrete slab. For this purpose, after presenting the equations related to the blast load and also developing the relationship between the behavior of concrete and reinforcement materials, the model validation will be investigated with and experimental research and two numerical studies in LS-DYNA software. It should be noted the blast load is applied to the structure in a very short time and the loading rate is high. Therefore, the strain rate effects on concrete and reinforcement are taken into account for achieving real material behavior. The following is intended to compare the behavior of slabs and the volume of concrete. The reinforcement materials in all slabs are similar and then the effect of the geometric dimensions of the waffle molds will be

examined. The other case which is examined is the effect of supporting condition on the waffle slab response. The effect of concrete compressive strength on the behavior of the slab under blast load is also studied. The mass of the explosive and its distance from the slab surface will be other parameters considered in this study. Besides the effect of bar size on slab behavior is examined.

2. Introducing the Blast Load

The blast phenomenon is caused by the rapid release of large amounts of energy in a confined space. In the engineering literature, researchers classify the blast in terms of location into two categories of indoor and outdoor blasts. The sudden release of energy creates a pressure wave in the environment that gradually decreases with a short period of time (Figure 1).

After the occurrence of blast in a short time, the pressure will reach its maximum. In the literature, the pressure due to the pressure difference between the blast

pressure and the atmospheric pressure is called pre-pressure. Over the time, the pressure gradually decreases until the blast pressure reaches the atmospheric pressure and this decreasing trend will continue and so-called suction will occur. Thus, the pressure-time diagram includes both positive and negative zones (Figure 2).

A criterion is introduced for determining the degradation severity as a mass-distance scale (Z_G) as follows:

$$Z_G = \frac{R}{\sqrt[3]{M}} \quad (1)$$

where R : is the distance from the blast point and M : is the mass of the explosive equivalent to TNT. The ambient air under the blast is considered an Expression of State (EOS) model. The pressure due to the blast in the environment is calculated from the following relation:

$$P = (\gamma - 1)\rho e \quad (2)$$

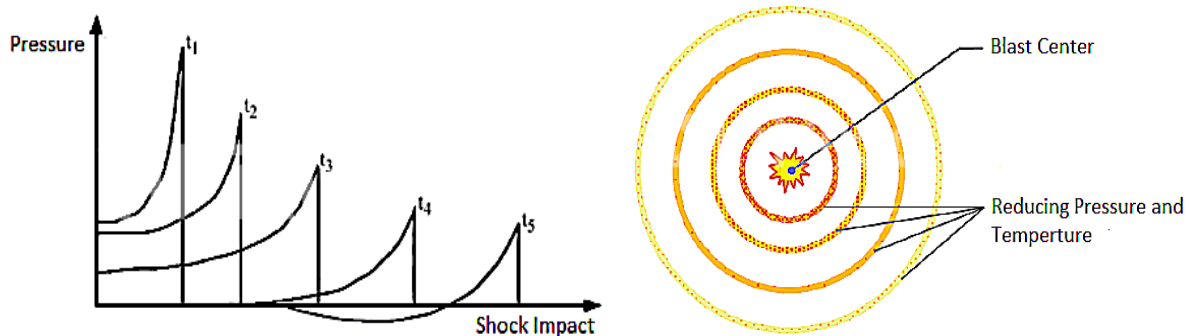


Fig. 1. Reduction of blast pressure over distance

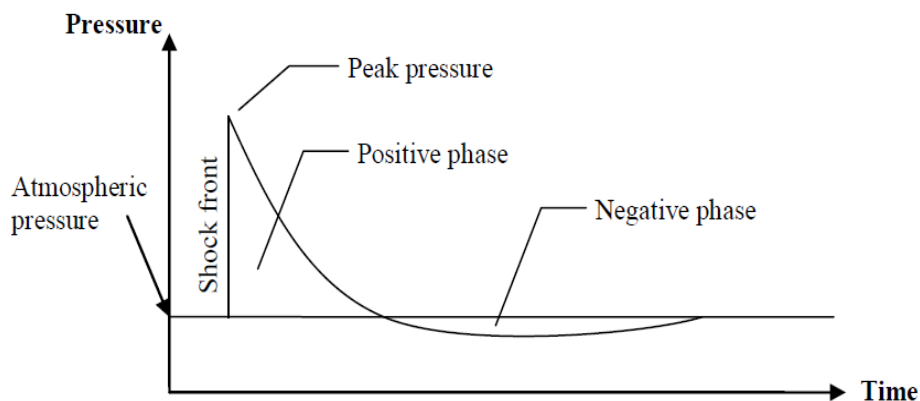


Fig. 2. Idealized shockwave pressure in time (Augustsson and Harenstam, 2010)

where, γ : is the constant value, ρ : is the density of air and e represents the internal energy. In this study, standard air constants are extracted from the library values in (LS-DYNA, 2006) where $\rho = 1.225 \text{ kg/m}^3$ and $\gamma = 14$. The initial internal energy of the air in the above equation is $e = 2.068 \times 10^5 \text{ KJ/kg}$. Explosives such as TNT are considered to be the Jones-Wilkins-Lee EOS model, which represents the pressure resulting from the chemical energy of a blast and is calculated as follows:

$$P = A \left(1 - \frac{\omega}{R_1 V} \right) e^{-R_1 V} + B \left(1 - \frac{\omega}{R_2 V} \right) e^{-R_2 V} + \frac{\omega E}{V} \quad (3)$$

where P : represents the hydrostatic pressure, V : is the specific volume of TNT, and A , B , R_1 , R_2 and ω : are constant values of the material. These constant values have been calculated for several blast samples from dynamic laboratory studies, which are referred to in (LS-DYNA, 2006). In this study, the values A , B , R_1 , R_2 and ω are $3.7377 \times 10^5 \text{ Mpa}$, 4.15 , $3.747 \times 10^3 \text{ Mpa}$, 0.9 and 0.35 respectively, for TNT explosives.

3. Characteristics of Materials

In order to obtain the most accurate results, the failure of the material such as concrete under the dynamic load of the blast should be appropriately modeled. Blast loads will

affect the behavior of the materials because they are applied to the structure in a very short time and have high loading rates. Therefore, the strain rate effects and inertia on the behavior of concrete and rebar should be taken into account because the higher strain rate increases the strength of such materials (Chen et al., 2015).

The concrete stress tensor is defined as sum of the hydrostatic stress tensor and the deviated stress tensor. The hydrostatic tensor shows the volume changes of the concrete and the deviated tensor shows the concrete deformation (Zhao and Chen, 2013).

In this study, the dynamic failure model of Riedel, Hiermaier and Thoma (RHT) for concrete has been considered. This model is very suitable for studying dynamic behavior of concrete. The RHT model is generally used for brittle materials and includes several features for various mechanisms in the field, including strain hardening, strain rate hardening, pressure hardening, third invariant dependence for tensile and compressive meridians and cumulative damage (strain softening). Conjunction with the existing tensile crack softening algorithm can be used in this model. The p - α equation of state for volumetric compaction is also considered in this model. As can be seen in Figure 3, the material has three strength surfaces including an elastic limit surface, a failure surface, and the remaining strength surface for the crushed material. For the elastic strength surface, a threshold often exists (Wang et al., 2013).

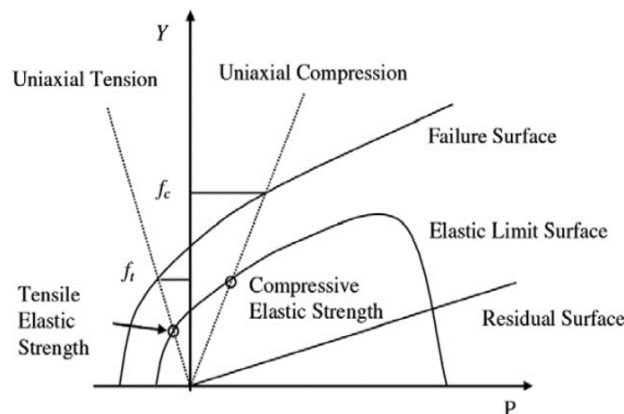


Fig. 3. Ultimate strength, yield strength and residual strength surfaces (Wang et al., 2013)

In Figure 3, Y : is the failure surface and defined as a function of pressure P , strain rate $\dot{\epsilon}$ and the load angle θ .

$$Y_f = Y_{(p)} \cdot R_{(\theta)} \cdot F_{RATE(\dot{\epsilon})} \quad (4)$$

where $Y_{(p)} = f_c \left[A(p^* - p_{spall}^* F_{RATE(\dot{\epsilon})})^N \right]$, with f_c : being the compressive strength, A : the failure surface exponent and p^* : the pressure normalized by f_c , $p_{spall}^* = p^*(f_t / f_c)$. $F_{RATE(\dot{\epsilon})}$: shows the strain rate function. $R_{(\theta)}$: represents the third invariant dependency of the model as a function of a meridian ratio Q_2 and the second and third stress invariants.

Figure 4 shows the compressive meridian on the stress π plane and the tensile. From the failure surface, the elastic limit surface is scaled as (Wang et al., 2013).

$$Y_e = Y_f \cdot F_e \cdot F_{CAP(p)} \quad (5)$$

where $F_{CAP(p)}$: is a function that limits the elastic deviatoric stresses under hydrostatic compression which is varying within the range of 0 to 1 for pressure. In this range, value 0 is initial compaction and 1 is solid compaction pressures. F_e : is the ratio of the elastic strength to failure surface strength. A residual (frictional) failure surface is defined as following equation (Wang et al., 2013).

$$Y_{residual}^* = B \cdot p^{*M} \quad (6)$$

where B : is the constant of residual failure surface and M : is the exponent of residual failure surface. It should be explained that additional plastic straining of the material results in damage and strength reduction after the hardening phase. Damage in the material is accumulated by:

$$D = \sum \frac{\Delta \epsilon_p}{\epsilon_p^{failure}} = \sum \frac{\Delta \epsilon_p}{D_1(p^* - p_{spall}^*)^{D_2}} \quad (7)$$

where D_1 and D_2 : are damage constants and the post-damage failure surface is then interpolated by:

$$Y_{fracture}^* = (1 - D)Y_{failure}^* + DY_{residual}^* \quad (8)$$

and the material post-damage shear modulus is interpolated via the following equation:

$$G_{fracture} = (1 - D)G_{initial} + DG_{residual} \quad (9)$$

where $G_{initial}$, $G_{residual}$, $G_{fracture}$: are the shear modulus. In the present work, the material constant is based on the typical data for concrete, which compressive strength, $f_c = 39.5$ Mpa and the material parameters are: shear modulus, $G = 0.28$ Mpa; reference density, $\rho = 2.55$ g/cm³; tensile strength, $f_t = 4.2$ Mpa; and A, N, B, M, D_1, D_2 and ϵ_f^{min} are 1.6, 0.61, 0.7, 0.8, 1, and 0.0008, respectively. Also, the failure strain is $\epsilon_f^{min} = 0.001$.

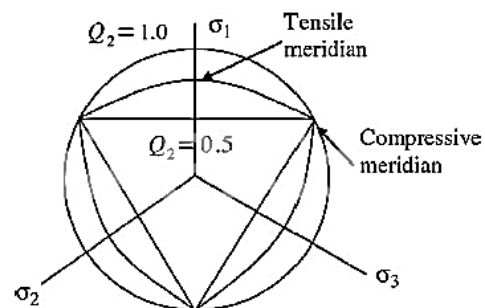


Fig. 4. The stress π plane (Wang et al., 2013)

Specifications of materials in software should be close to the behavior of materials in experimental research. The Abaqus software considers three behavioral models for concrete, including Concrete Smeared Cracking, Brittle Cracking, and Concrete Damaged Plasticity model. In this study, the Concrete Damaged Plasticity model is used because it is close to the actual concrete behavior model. The coefficient of increase of dynamic compressive and tensile strength of concrete is calculated using Eqs. (10-13) (Chen et al., 2015).

$$CDIF = \frac{f_c}{f_{cs}} = \left(\frac{\dot{\epsilon}}{\dot{\epsilon}_{cs}} \right)^{1.026\alpha} \quad \text{if } \dot{\epsilon} \leq 30s^{-1} \quad (10)$$

$$CDIF = \frac{f_c}{f_{cs}} = \gamma(\dot{\epsilon})^{1/3} \quad \text{if } \dot{\epsilon} > 30s^{-1} \quad (11)$$

$$TDIF = \frac{f_t}{f_{ts}} = \left(\frac{\dot{\epsilon}}{\dot{\epsilon}_{ts}} \right)^\delta \quad \text{if } \dot{\epsilon}_{td} \leq 1s^{-1} \quad (12)$$

$$TDIF = \frac{f_t}{f_{ts}} = \beta = \left(\frac{\dot{\epsilon}}{\dot{\epsilon}_{ts}} \right)^{1/3} \quad \text{if } \dot{\epsilon}_{ts} > 1s^{-1} \quad (13)$$

where f_c : is the dynamic concrete compressive strength at strain rate of $\dot{\epsilon}$, f_{cs} : represents the concrete static compressive strength at strain rate of $\dot{\epsilon}_{cs}$, $\log \gamma = 6.156\alpha - 0.49$, $\alpha = 1/(5 + 3f_{cu}/4)$ and f_{cu} : denotes the compressive strength of the cube concrete sample in MPa. f_t : is the concrete dynamic tensile strength at the strain rate of $\dot{\epsilon}$ is assumed to be within the range of $1 - 5 \cdot 10^{-6} S^{-1}$ to $160 S^{-1}$, f_{ts} the concrete tensile strength at the strain rate of $\dot{\epsilon}_{ts}$, $\log \beta = 6\delta - 2$, $\delta = 1/(1 + 8f'_c/f'_{co})$ and f'_{co} is equal to 10 MPa (Chen et al., 2015).

Johnson-Cook behavior model has been considered for rebar because it is suitable for studying the behavior of material under high strain rate and heat. This model defines rebar yield stress Y as (Johnson and Cook, 1983):

$$\sigma = \left[A + B\varepsilon_p^n \right] \left[1 + C \ln \frac{\dot{\epsilon}_p}{\dot{\epsilon}_0} \right] \left[1 - T_H^m \right] \quad (14)$$

where, ε_p : represents the effective plastic strain, $\dot{\epsilon}_p^* = \frac{\dot{\epsilon}}{\dot{\epsilon}_0}$ is equal to the effective plastic strain rate for $\dot{\epsilon}_0 = 1s^{-1}$, $T_H = (T - T_{room}) / (T_{melt} - T_{room})$, where T_{room} represents the room temperature and T_{melt} : is the melting temperature and also A , B , C , n and m : are the five material constant (Johnson and Cook, 1983). The density of rebar used in this study is equal to $\rho = 7.85 \text{ g/cm}^3$, bulk modulus is $K = 159 \text{ Gpa}$ and

shear modulus is $G = 81.8 \text{ Gpa}$. The coefficient of increase of the dynamic strength of the steel (DIF) is calculated from the Eq. (15), where f_y represents the yielding strength of the rebar in MPa.

$$DIF = (\dot{\epsilon} / 10^{-4})^\alpha \quad (15)$$

$$\alpha = 0.074 - 0.04f_y / 414$$

4. Modeling

In this study, simulation of reinforced concrete slab and waffle slab under blast load was performed in ABAQUS software. Solid element was used for modeling concrete and Concrete Damaged Plasticity model was used for concrete material behavior in software. In this model, the effects of strain rate and crack on concrete elements are considered. Beam element was used in the rebar and also Johnson-Cook plastic model capable of considering strain rate was used for the behavior of steel material. To model the contact between the concrete and the reinforcements, it was assumed that the reinforcements were buried in the concrete. Therefore, the Embedded region model was used in the software to contact between the two materials. In the blast loading, the loading speed is high and the slip between the concrete and the reinforcements can be neglected. This behavioral model does not take into account the slip between the two materials (Xu and Lu, 2006).

To ensure the accuracy of the simulation performed in ABAQUS software, the results of the experimental model performed by Wang et al. (2013) and the numerical models performed in LS-DYNA software by Zhao et al. (2013) and (Shuaib and Daoud (2015), which a $1000 \times 1000 \times 40$ mm reinforced concrete slab, have been compared with the present study. In these studies, the reinforcements are meshed in a row with a diameter of 6 mm at 75 mm intervals. The concrete cover is 20 mm and the compressive strength, tensile strength and modulus of elasticity of concrete are

39.5 MPa, 4.2 MPa and 28.3 Gpa, respectively. The yield stress of the reinforcement is also assumed to be 600 MPa and its modulus of elasticity is 200 Gpa. Figure 5 shows an image of the experimental and numerical model made in Wang et al. (2013), Zhao and Chen (2013) and Shuaib and Daoud (2015).

An illustration of the reinforced concrete

slab studied has been shown in Figure 6. As shown in this figure, the explosive is located above the slab 400 mm from the center of the slab and its mass is 0.46 kg.

Figure 7 illustrates an image of the blast load applied to the RC slab at the RP-1 point as a CONWEP blast model in ABAQUS software. Also, the deformed RC slab is presented in Figure 8.

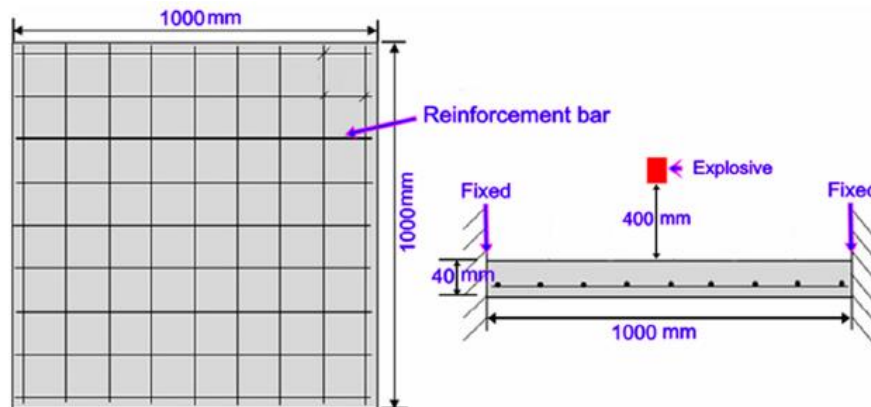


Fig. 5. The geometry of the reinforced concrete slab studied in experimental and numerical references (Wang et al., 2013; Zhao and Chen, 2013; Shuaib and Daoud, 2015)



Fig. 6. Laboratory specimen of reinforced concrete slab in reference (Wang et al., 2013)

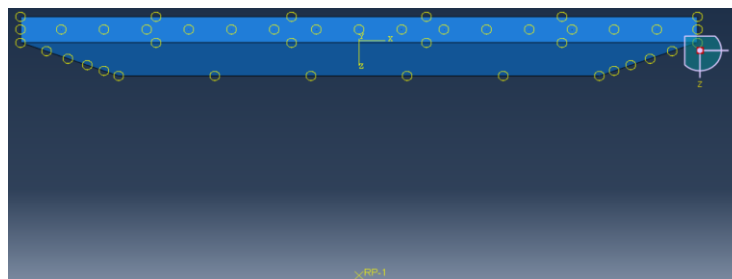


Fig. 7. Applying the blast load to the RC slab at RP-1 point

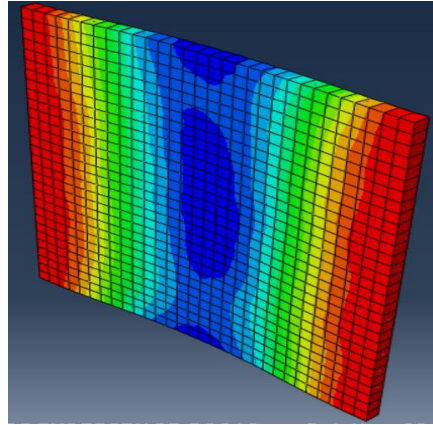


Fig. 8. Deformation of RC slab after blast loading

As is observed in Figure 9, the magnitude of the slab center displacement due to the blast load has a negligible difference with the results obtained from Wang et al. (2013), Zhao and Chen (2013) and Shuaib and Daoud (2015), indicating the accuracy of the modeling performed in ABAQUS software. Now, after verifying the accuracy of the modeling, the behavior of the waffle slab under the blast load is investigated. For this purpose, in order to compare the behavior of the waffle slab with the RC slab subjected to the blast load, a RC slab with dimensions of 5000×5000×200 mm is first considered.

The reinforcement in this slab is in the form of mesh in a row with 12 mm diameter and 300 mm intervals. The specifications of the concrete and reinforcement are the same as in the previous slab. In order to uniformize the conditions in terms of volume of concrete and reinforcement materials used in RC slab and waffle slab, the geometrical characteristics of the desired waffle slab are as in Figure 10. The three-dimensional image in ABAQUS software can be seen in Figure 11. It should be noted that the characteristics of the material used in the waffle slab are the same as in the previous specifications.

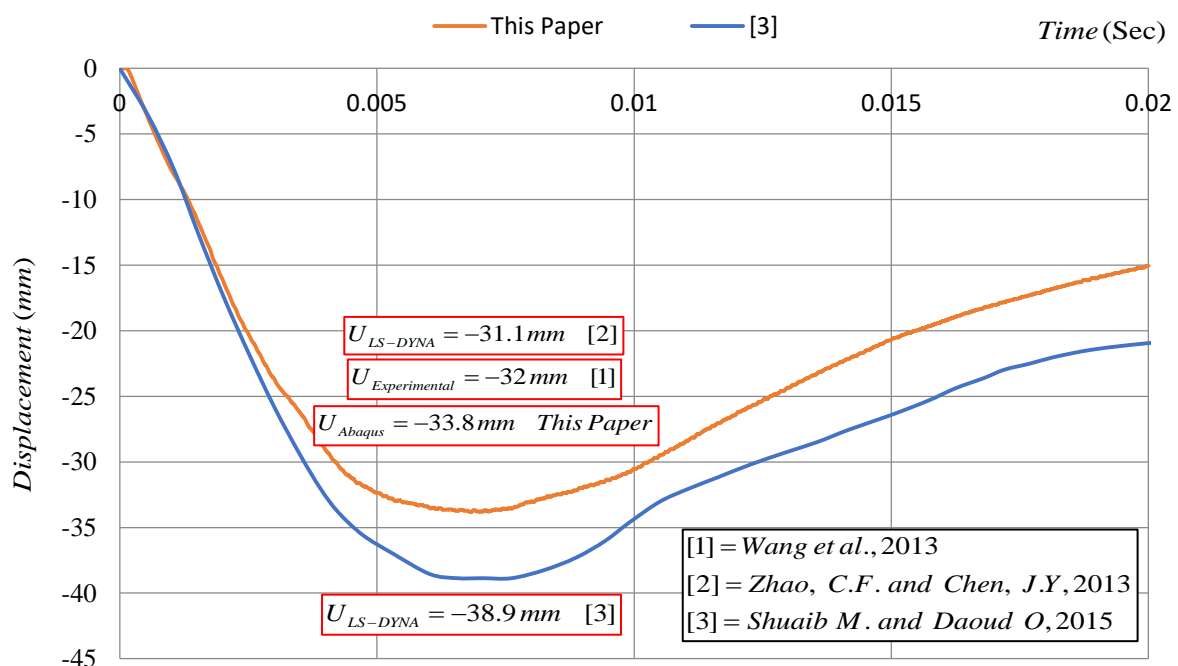


Fig. 9. Comparison of slab center displacement values in ABAQUS software with experimental study and numerical study in LS-DYNA software

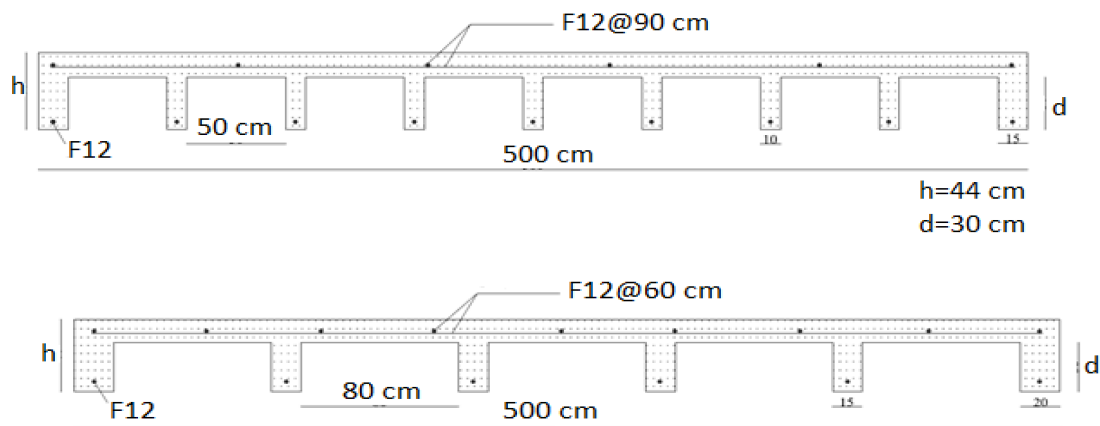


Fig. 10. Geometric properties of waffle slab with molds dimensions of 50×50×30 cm and 80×80×30 cm

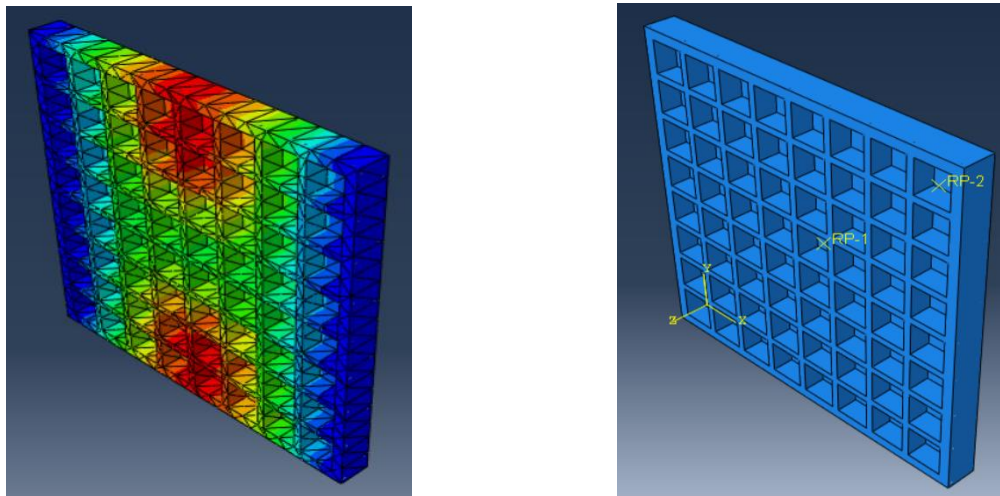


Fig. 11. Three-dimensional view of the waffle slab with molds dimension of 50×50×30 cm

Figure 12 shows a comparison of the displacement of the center of the RC slab and the waffle slab over time. In this comparison, both slabs have two fixed-supported sides, the volume of concrete and reinforcement are same and the mass of TNT is 0.5 kg that is located 2 m from the center of the slabs. As can be seen in this figure, waffle slab shows lower displacement under the blast load. As illustrated in Figure 13, studies on the effect of molds dimensions of waffle slab show that with the same volume of concrete and reinforcement materials, the molds dimensions have little effect on the behavior of the slab under the blast load. Three cases have been considered to investigate the effect of supporting conditions on the behavior of the waffle slab. The first case with two sides of the slab with fixed support (2 Fixed), the second case with four sides of

the slab with fixed support (4 Fixed) and the third case with four pinned support sides (4 Pinned).

As can be seen in Figure 14, the displacement of the center of the slab in the second and third cases is less than the first case, indicating that fixing four sides of the slab offers better responses than fixing two sides of the slab and it can reduce the displacement of the slab center. Another point which is evident in this figure is that the type of slab support does not have an effect on the displacement of the center of the slab due to the blast load. In other words, it could show that the damage of the slab under blast has been localized and boundary condition cannot reduce the displacement and therefore local damage to the slab.

Figure 15 presents the effect of concrete compressive strength on the displacement of the center of the slab, which shows that

the slab displacement decreases as the concrete compressive strength increases. It is noteworthy in this figure that the restriction of slab displacement by increasing the strength of concrete decreases its effect approximately from the concrete grade C45 to above. Table 1 shows the effect of the explosive mass on the maximum displacement of the center of the waffle slab. For this purpose, the distance of the blast position is fixed at 2 m, but the mass of the explosive increased from 0.25 kg to 2.5 kg. The results show that with increasing mass of the explosive, the displacement of the center of the slab also

increases.

Table 2 shows the effect of explosive distance on the maximum displacement of the center of the waffle slab. Therefore, the mass of the explosive is considered to be constant and equal to 1 kg and its distance varies. The results show that by increasing the distance of the explosive from the center of the slab, the displacement of the center of the slab is reduced. Finally, Figure 16 illustrates the effect of reinforcement size on the displacement of the center of the waffle slab for C30 concrete and the slab on two fixed sides subjected to the explosive with mass of 0.5 kg at a distance of 2 m.

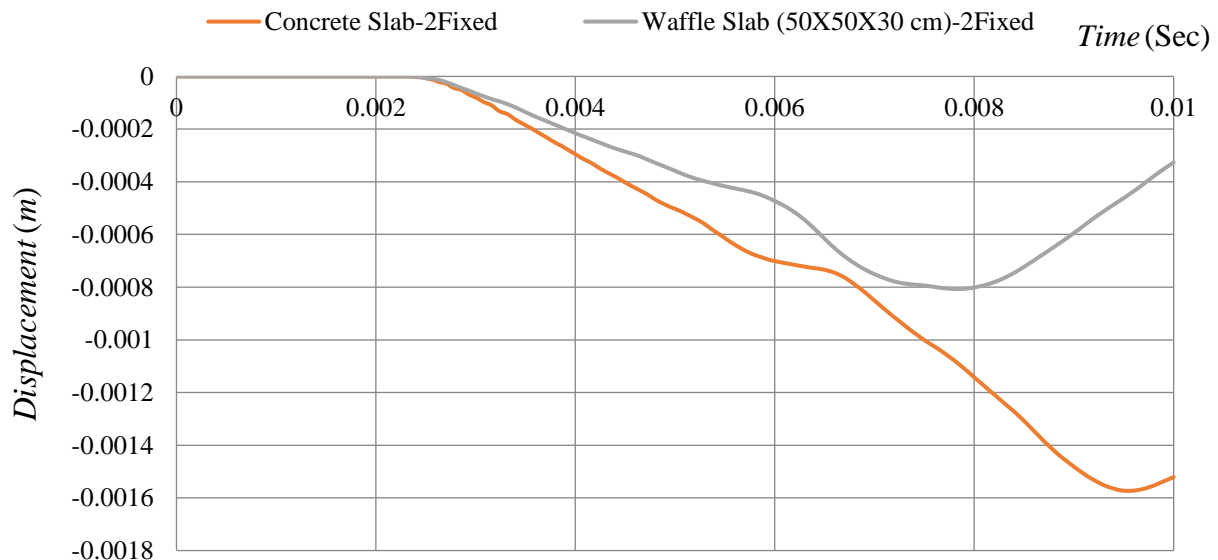


Fig. 12. Comparison of the displacement of the center of RC slab and waffle slab with waffle molds dimension of 50×50×30 cm

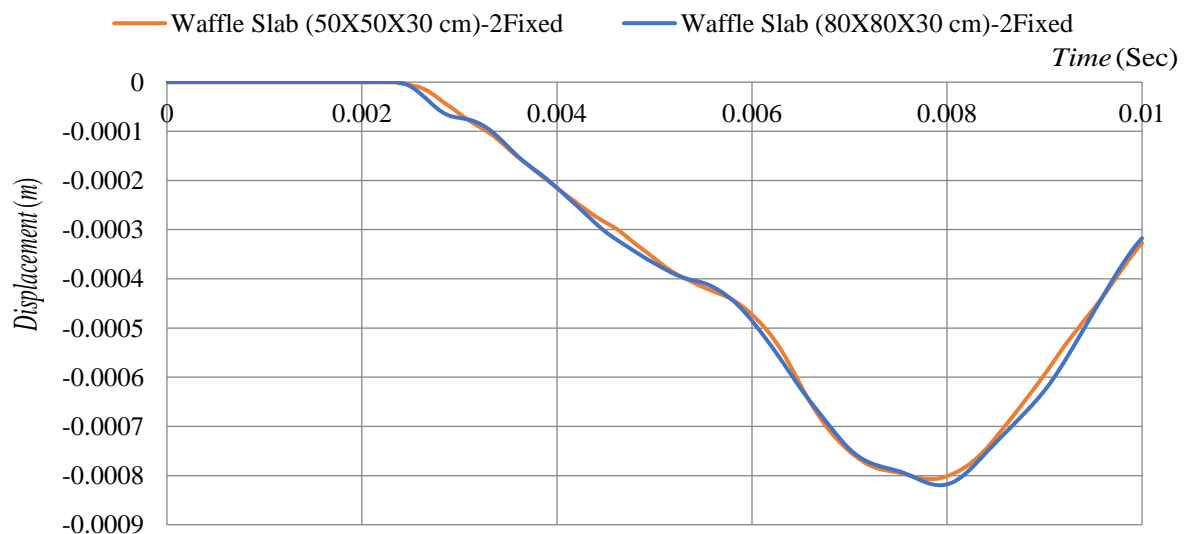


Fig. 13. Comparison of the displacement of the center of waffle slab with the molds dimensions of 50×50×30 cm and 80×80×30 cm

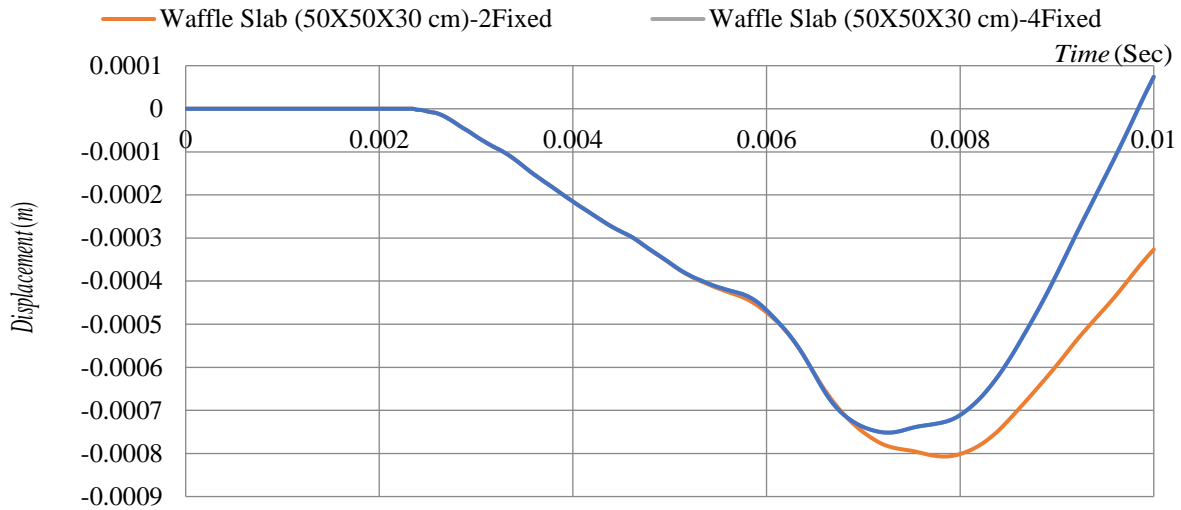


Fig. 14. Effect of supporting conditions on the displacement of the center of waffle slab with molds dimension of 50×50×30 cm

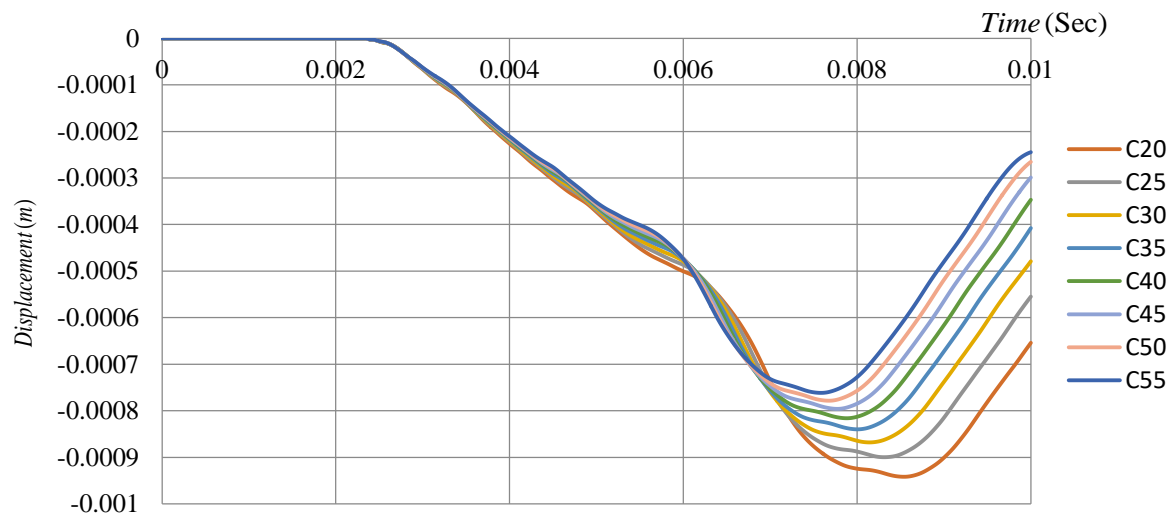


Fig. 15. Effect of compressive strength of concrete on the displacement of center of waffle slab with molds dimension of 50×50×30 cm

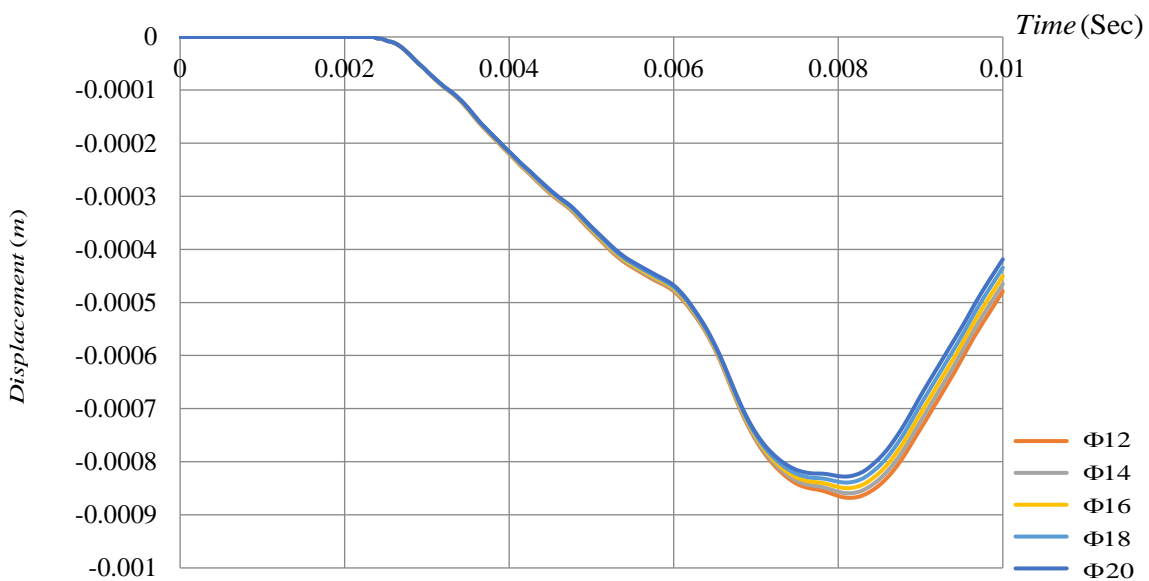


Fig. 16. Effect of reinforcement size on the displacement of center of waffle slab with molds dimension of 50×50×30 cm and C30 concrete

Table 1. Effect of explosive mass on the maximum displacement of the center of the waffle slab with molds dimension of 50×50×30 cm and C30 concrete

Z_i	R_i (m)	M_i (Kg)	U_{iMax} (m)
$Z_1=3.1748$	$R_1=2$	$M_1=0.25$	$U_1=0.0005$
$Z_2=2.5198$	$R_2=2$	$M_2=0.5$	$U_2=0.0009$
$Z_3=2.2013$	$R_3=2$	$M_3=0.75$	$U_3=0.0012$
$Z_4=2$	$R_4=2$	$M_4=1$	$U_4=0.0015$
$Z_5=1.8566$	$R_5=2$	$M_5=1.25$	$U_5=0.0018$
$Z_6=1.7472$	$R_6=2$	$M_6=1.5$	$U_6=0.0021$
$Z_7=1.6597$	$R_7=2$	$M_7=1.75$	$U_7=0.0024$
$Z_8=1.5874$	$R_8=2$	$M_8=2$	$U_8=0.0026$
$Z_9=1.5263$	$R_9=2$	$M_9=2.25$	$U_9=0.0029$
$Z_{10}=1.4736$	$R_{10}=2$	$M_{10}=2.5$	$U_{10}=0.0032$

Table 2. Effect of explosive distance on the maximum displacement of the center of the waffle slab with molds dimension of 50×50×30 cm and C30 concrete

Z_i	R_i (m)	M_i (Kg)	U_{iMax} (m)
$Z_1=3.1748$	$R_1=3.1748$	$M_1=1$	$U_1=0.00090$
$Z_2=2.5198$	$R_2=2.5198$	$M_2=1$	$U_2=0.00115$
$Z_3=2.2013$	$R_3=2.2013$	$M_3=1$	$U_3=0.00130$
$Z_4=2$	$R_4=2$	$M_4=1$	$U_4=0.0015$
$Z_5=1.8566$	$R_5=1.8566$	$M_5=1$	$U_5=0.00151$
$Z_6=1.7472$	$R_6=1.7472$	$M_6=1$	$U_6=0.00158$
$Z_7=1.6597$	$R_7=1.6597$	$M_7=1$	$U_7=0.00164$
$Z_8=1.5874$	$R_8=1.5874$	$M_8=1$	$U_8=0.00169$
$Z_9=1.5263$	$R_9=1.5263$	$M_9=1$	$U_9=0.00174$
$Z_{10}=1.4736$	$R_{10}=1.4736$	$M_{10}=1$	$U_{10}=0.00179$

5. Conclusions

This study investigated the behavior of the waffle slab under the blast load and comparison of its performance with that of conventional reinforced concrete slab. For this purpose, after presenting the equations related to the blast load, and the formulation of behavior of concrete and reinforcement materials, the model validation was also investigated by experimental research and two numerical studies in LS-DYNA software. Because the blast load was applied to the structure in a very short time, the loading speed was high. Therefore, the effects of strain rate on concrete and reinforcement were taken into account for achieving real behavior of the materials.

In order to study and compare rationally the behavior of slabs, the volume of concrete and reinforcement materials in all slabs was considered similar and then the effect of geometric dimensions of the molds was investigated. In addition, the effect of supporting conditions on the responses of the waffle slab and the effect of compressive strength of the concrete on the

behavior of the slab under the effects of blast were also studied. The explosive mass and its distance from the slab were the other parameters considered in this study. The effect of reinforcement size on the behavior of the slab under blast was also investigated. The following items can be mentioned as the important results of this research:

- Comparing the results of this study as a numerical simulation in ABAQUS software with the results of experimental studies, it is evident that the investigation of blast effects on the slab in numerical simulation had desirable accuracy and this method of study can be a good substitute for experimental methods which require a great deal of precision, time and cost.
- The investigations in this research illustrate that under the same conditions of materials such as concrete and reinforcement and their volume, the waffle slab shows less displacement and better behavior than those of conventional reinforced concrete slab under blast load. The increase in moment of inertia in the waffle slab is one of the

most important reasons for better behavior under the blast load.

- Under the same conditions of volume of concrete and reinforcement materials, the results show that the geometrical dimensions of the molds have little effect on the slab responses under the blast load.
- Based on the studies on the effects of the slab support conditions, in the case where the slab is fixed at all four sides a better response under the blast load compared to the case with two fixed sides is achieved. The important conclusion of this study is that changing the type of support from the fixed type to the pinned type does not have much effect on the slab responses, which could be due to the high blast loading rate. Because the slab failure under blast will occur rapidly and locally in the center of the slab and the support does not have enough time to show its effects on the slab response.
- As the compressive strength of concrete increases, the slab response also improves as the slab center displacement decreases with increasing concrete compressive strength. But the slope of the ratio of changes from C45 concrete grade upwards gradually decreases.
- Investigations on the effect of mass and distance of the explosive show that for a given distance from the blast point to the center of the slab, as the mass of the explosive increases, the destruction effects on the slab increase. Also, for a given mass of explosive, as the blast point distance to the slab shortens, the slab center displacement and slab demolition effects increase, which is conceivable. Two scenarios in this study have been investigated for a given amount of mass-distance scale. The first scenario is with a mass of 0.25 kg at a distance of 2 m and the second scenario with a mass of 1 kg at a distance of 3.1748 m that the mass-distance scale for both scenarios is 3.1748. But the interesting conclusion is that the second

scenario leads to higher displacement and consequently more slab damage. This result means that for the identical mass-distance scale, the mass value has a greater effect on the slab behavior than the distance value from the blast point to the slab.

- Studies on the effect of reinforcement size on the behavior of the waffle slab subjected to the blast show that with increasing rebar size, the displacement of the center of the slab decreases. But its impact is not significant compared to concrete, indicating that reinforcement is less effective than concrete on the waffle slab responses subjected to blast.

6. References

- Abdollahzadeh, G.R., Jahani, E. and Kashir, Z. (2017). "Genetic programming-based formulation to predict compressive strength of high strength concrete", *Civil Engineering Infrastructures Journal*, 50(2), 207-219.
- Augustsson, R. and Harenstam, M. (2010). "Design of reinforced concrete slab with regard to explosion", M.Sc. Thesis, Department of Civil and Environmental Engineering, Chalmers University of Technology, Göteborg, Sweden.
- Chen, W., Hao, H. and Chen, S. (2015). "Numerical analysis of prestressed reinforced concrete beam subjected to blast loading", *Materials and Design*, 65, 662-674.
- Eltehawy, E. (2009). "Effect of using ferro-cement on the mechanical properties of reinforced concrete slab subjected to dynamic loads", *Aerospace Sciences a Aviation Technology*, ASAT-13, 26-28.
- Johnson, G.R. and Cook, W.H. (1983). "A constitutive model and data for METALS subjected to large strain, high strain rates and high temperatures", *Proceedings of the Seventh International Symposium on Ballistics, The Hague, The Netherlands*, 541-548.
- Kheyroddin, A., Sharbatdar, M.K. and Farahani, A. (2019). "Effect of structural height on the location of key element in progressive collapse of RC structures", *Civil Engineering Infrastructures Journal*, 52(1), 41-58.
- LS-DYNA. (2006). "Theory manual", Compiled by John O. Hallquist, Livermore Software Corporation, Livermore, California.
- Meng, Q., Wu, Ch., Su, Y., Li, J., Liu, J. and Pang, J. (2019). "A study of steel wire mesh reinforced high performance geopolymer concrete slabs under blast loading", *Journal of Cleaner Production*, 210, 1150-1163.

- Pandey, A.K., Kumar, R., Paul, D.K. and Trikha, D.N. (2006). "Non-linear response of reinforced concrete containment structure under blast loading", *Nuclear Engineering and Design*, 236, 993-1002.
- Rezaie, F., Fakhradini, S.M. and Ghahremannejad, M. (2018). "Numerical evaluation of progressive collapse potential in reinforced concrete buildings with various floor plans due to single column removal", *Civil Engineering Infrastructures Journal*, 51(2), 405-424.
- Shuaib, M. and Daoud, O. (2015). "Numerical modelling of reinforced concrete slabs under blast loads of close-in detonations using the lagrangian approach", *Journal of Physics: Conference Series*, 628 (1), 1-8.
- Tavakoli, H.R. and Kiakojouri, F. (2015). "Threat-independent column removal and fire-induced progressive collapse: Numerical study and comparison", *Civil Engineering Infrastructures Journal*, 48(1), 121-131.
- Wang, W., Zhang, D., Lu, F., Wang, S.C. and Tang, F. (2013). "Experimental study and numerical simulation of the damage mode of a square reinforced concrete slab under close-in explosion", *Engineering Failure Analysis*, 27, 41-51.
- Xu, K. and Lu, Y. (2006). "Numerical simulation study of spallation in reinforced concrete plates subjected to blast loading", *Computers and Structures*, 84, 431-438.
- Yang, F., Feng, W., Liu, F., Jing, L., Yuan, B. and Chen, D. (2019). "Experimental and numerical study of rubber concrete slabs with steel reinforcement under close-in blast loading", *Construction and Building Materials*, 198, 423-436.
- Zahrai, S.M. and Ezoddin, A.R. (2014). "Numerical study of progressive collapse in intermediate moment resisting reinforced concrete frame due to column removal", *Civil Engineering Infrastructures Journal*, 47(1), 71-88.
- Zhao, C.F. and Chen, J.Y. (2013) "Damage mechanism and mode of square reinforced concrete slab subjected to blast loading", *Theoretical and Applied Fracture Mechanics*, 63-64, 54-62.
- Zhao, Ch., Lu, X., Wang, Q., Gautam, A., Wang, J. and Mo, Y.L. (2019). "Experimental and numerical investigation of steel-concrete (SC) slabs under contact blast loading", *Engineering Structures*, 196, 1-13.



This article is an open-access article distributed under the terms and conditions of the Creative Commons Attribution (CC-BY) license.